Integrating Multiple Textural Features for Remote Sensing Image Change Detection

Qingyu Li, Xin Huang, Dawei Wen, and Hui Liu

Abstract

This paper proposes a multi-texture change detection method by integrating macro- and micro-texture features. Macro-textures are related to the information defined by the whole image scene, while micro-textures describe distributions and relationships of the gray levels within a local window. Moreover, we propose two strategies, random forests (RF) and a fuzzy set model, to integrate different characteristics of the textures. Experiments were conducted on ZY-3 *(the first civilian high-resolution stereo mapping satellite of China) orthographic images of the cities of Wuhan and Tokyo, as well as WorldView-2 multi-spectral images of the city of Kuala Lumpur. Results showed that the wavelet-based features obtained the highest accuracy among the macro-textures, while the morphological attributes obtained the best results for the micro-textures. By integrating both micro- and macro-textures, the texture combination using both RF and a fuzzy set model can further improve the accuracy of change detection.*

Introduction

Multi-temporal change detection is one of the most important techniques for remote sensing applications. As a result, it has been extensively applied in various aspects for dynamically monitoring and acquiring the trend of land evolution. A large number of the existing approaches for remote sensing change detection are based on spectral comparison between multi-temporal images. These approaches, such as image differencing (Al-Khudhairy, 2005), image rationing (Im and Jensen, 2011), change vector analysis (CVA) (Chen *et al.*, 2003), vegetation index differencing (Sohl, 1999), post-classification comparison (Homer *et al.*, 2015), artificial neural networks (ANNs) (Liu and Lathrop Jr., 2002), and support vector machine (SVM) (Zhang *et al.*, 2012), regard a single pixel as the basic processing unit.

However, although the pixel-based and spectral-based methods are widely used for remote sensing image change detection, they have the following deficiencies:

1. Pixel-based change detection neglects the neighboring pixels and does not consider the spatial correlation when determining whether or not a pixel has changed (Johansen *et al.*, 2010).
2. Spectral-based change detection overlooks the textural and structural characteristics of the images. When considering the spectral information alone, the results may not be satisfactory for the change detection of remote sensing data (Huang and Zhang, 2012), since the high intra-class variation and low inter-class variation can lead to inadequacy and uncertainty of the pattern analysis in the spectral domain (Huang and Zhang, 2013). Furthermore, this problem becomes more serious when processing high-resolution remote sensing imagery (Huang and Zhang, 2013).

In this context, the textural information has recently been considered in change detection in order to exploit spatial information to complement and enhance the spectral-based and pixel-based methods. Transform-based textures are among the most commonly used textures for change detection. In Klonus *et al.* (2012) and Aghababaee *et al.* (2012), multi-temporal images were transformed by the use of a fast Fourier transform, and the most suitable band-pass filter was applied to extract the changed structures. The extended transforms, such as curvelet and contourlet, have also been proved to have better shift-invariance property and directional selectivity (Li *et al.*, 2014). Gray level co-occurrence matrix (GLCM) has also been considered in texture-based change detection (He *et al.*, 2011). Moreover, in recent years, morphological textures have attracted much attention for change detection, and it has been shown that morphological operators are appropriate for describing the structural change of high-resolution images by taking into account spatial and structural correlation (Dalla Mura *et al.*, 2008). Another example of texture-based change detection is the fractal method. For instance, in Huang *et al.* (2011) and Aghababaee *et al.* (2012), the fractal method was used for multi-temporal SAR change detection. Another fractal measure, lacunarity, was also used to detect slum area change in Hyderabad, India, using QuickBird and WorldView-2 imagery (Kit and Lüdeke, 2013).

Although a number of the existing papers have attempted texture-based change detection, they only took a specific kind of texture into consideration and neglected the comparison and combination of different textures in change detection. However, in fact, different textural features have different effects and performances in various image scenes. For instance, transform-based methods describe the macro-textures, while the GLCM and mathematical morphology focus on local structures. In this regard, one of the motivations of this study is to better understand the texture-based change detection methods by comparing and analyzing the performance and characteristics of different textures for image change detection. Moreover, it can be stated that a mono-texture is biased for image representation, as it is difficult to sufficiently describe the complex and varied geospatial targets using only one texture feature. Therefore, we propose to combine micro-textures (local structures) and macro-textures (global characteristics) for change detection, which has not been adequately addressed in the current literature. In addition, it should be noted that, in this research, a number of textures are exploited in change detection and analysis for the first time, such as the three-dimensional wavelet transform (3D-WT).

Xin Huang is with the School of Remote Sensing and Information Engineering, Wuhan University, Wuhan, China (corresponding author: Xin Huang, huang_whu@163.com).

Qingyu Li, Dawei Wen, and Hui Liu are with the State Key Laboratory of Information Engineering in Surveying, Mapping and Remote Sensing, Wuhan University, Wuhan, China (corresponding author: Dawei Wen, daweiwen@whu.edu.cn).

Photogrammetric Engineering & Remote Sensing
Vol. 83, No. 2, February 2017, pp. 109–121.
0099-1112/17/109–121

doi: 10.14358/PERS.83.2.109

The proposed multi-texture change detection method is described in the next Section 2, followed by experimental results and analyses. Next, a discussion is provided leading to conclusions.

Methodology

In this section, the first part briefly describes the adopted texture features for change detection. In the second part, the multi-texture fusion procedure for change detection is proposed.

Texture Features

The representative and state-of-the-art textural measures considered in this paper are listed in Table 1. All the selected texture features for change detection belong to four categories: (1) statistical textures, (2) structural textures, (3) model-based textures, and (4) transform-based textures. Please note that the textures that have not previously been applied to change detection are underlined in the Table 1.

1. Statistical Textures

Statistical textures describe the distribution and relationships of the gray levels of an image.

The most commonly used second-order statistical texture is the GLCM, which describes the joint probability distributions of pairs of pixels (Haralick *et al.*, 1973). It works by forming a moving window through the image and then calculating the frequency of co-occurrence for the pixel values in a defined number of directions (e.g., 0°, 45°, 90°, or 135°). Once the counting of the co-occurrence frequencies for all the pixels within the window has been completed, one can then compute statistical measures to extract texture features.

In this research, we also consider the pixel shape index (PSI) for change detection. It is a pixel-based feature which measures the gray similarity distance in every direction by defining a set of anisotropic direction lines radiating from the central pixel (Zhang *et al.*, 2006). A multi-feature version of the PSI based on direction lines was presented by Huang *et al.* (2007), where a set of structural features were used to classify high-resolution urban imagery.

2. Structural Textures

A good symbolic description of an image, such as well-defined primitives (micro-texture) or a hierarchy of spatial arrangements (macro-texture) of those primitives (Haralick *et al.*, 1973) can be provided by the structural texture, which attempts to explicitly understand the hierarchical structure of the texture (Materka and Strzelecki, 1998). A poweRFul and representative structural texture analysis approach is mathematical morphology (Serra, 1983). Mathematical morphology is based on rigorous mathematical theory and has been successfully applied to image processing and pattern recognition. With an aim of image analysis and recognition, it employs a set of structuring elements (SEs) with different shapes to measure and extract the image shape information.

A well-known morphological operator for remote sensing is morphological profiles (MPs), which are built by the use of openings and closings by reconstruction with a set of SEs of different sizes. MPs can preserve the geometrical characteristics of important regions and details (Dalla Mura *et al.*, 2010). Another variant of MPs, differential morphological profiles (DMPs), were proposed by Pesaresi and Benediktsson (2001) to represent differences of the MP values at different scales. MPs and DMPs are efficient in extracting image spatial information, but they do have limitations, e.g., SEs are of a fixed shape and are unable to capture the gray-level characteristics of the regions, such as homogeneity and contrast (Ghamisi *et al.*, 2015). To address these limitations, the concept of attribute profiles (APs) was proposed (Dalla Mura *et al.*, 2010), where a set of morphological attribute filters (AFs), such as area, moment of inertia, and standard deviation, were used to provide a multilevel characterization of the image.

3. Model-Based Textures

Model-based texture analysis is based on the construction of an image model that can be used to describe the texture and simultaneously synthesize it (Tuceryan and Jain, 1998). The parameters derived from the model are estimated and then implemented in image analysis (Materka and Strzelecki, 1998). In this study, the fractal dimension, which is a representative model-based texture, is used.

Fractal models are an effective and popular way of modeling statistical properties of roughness and self-similarity of natural suRFaces at different scales (Tuceryan and Jain, 1998).

Table 1. The Selected Textural Measures for Change Detection in This Research

Category of texture	Methods	Description	Characteristic
Statistical textures	GLCM	Local	Computes statistical measures based on the co-occurrence frequencies for the pixel values in a defined number of directions.
	PSI	Local	Measures the gray similarity distance in every direction by defining a set of anisotropic direction lines radiating from the central pixel.
Structural textures	MPs	Local	Extracts the image shape information by employing openings and closings by reconstruction with a set of structuring elements.
	DMPs	Local	Measures the slope of the opening-closing profiles for every step of the scale parameters.
	APs	Local	Provides a multilevel characterization of an image by the use of a set of morphological attribute filters, such as the area, the moment of inertia, and the standard deviation.
Model-based textures	Fractal	Local	Models the statistical properties of roughness and self-similarity of natural surfaces at different scales.
Transform-based textures	2D-WT	Macro	Extracts texture information from an image or a local moving window by using low-pass and high-pass filters in the spatial domain.
	3D-WT	Macro	Extracts texture information from an image or a local moving window by using low-pass and high-pass filters in both the spatial domain and spectral direction.
	Gabor	Macro	Provides a means for effective spatial and frequency localization through the Gaussian window transform.
	CT	Macro	Captures the geometrical details of the source image based on two-dimensional non-separable filter banks.

A number of methods have been proposed for estimating the fractal dimension, such as the box counting (Goodchild, 1980) and triangular prism (Clarke, 1986) methods. However, some studies have shown that the fractal dimension is unable to capture all the textural properties sufficiently, i.e., textures that have very similar fractal dimensions can be perceptually very different (Keller *et al.*, 1989). To this aim, Mandelbrot (1983) proposed another fractal measure, lacunarity, which represents the discrepancy between the actual mass and the expected value of the mass. It can describe the textural property more effectively and, hence, can be used to distinguish between different textures. The lacunarity fractal texture is therefore considered in this research.

4. Transform-Based Textures

Transform-based texture analysis methods aim to project an image into a new space whose coordinate system is closely connected with the characteristics of a texture (e.g., frequency and size) (Materka and Strzelecki, 1998). Representative transform-based textures include the Gabor texture feature (Daugman, 1975), wavelet transform (WT) (Mallat, 1989), and their extended forms.

Gabor filter is an orientation- and frequency-selective filter (Tuceryan and Jain, 1998), which provides a means for effective spatial and frequency localization through the Gaussian window transform. An important property of Gabor filters is that they have optimal joint localization in both spatial and spatial frequency domains (Daugman, 1975).

WT is a time-frequency method which represents an image from fine to coarse resolutions at any of the decomposition levels. It can extract texture information from an image or a local moving window by the use of low-pass and high-pass filters. Compared to the Fourier transform (Rosenfeld and Weszka, 1976), wavelet analysis is localized in space as well as in frequency, and allows for a better representation of an image. It can therefore represent features at the most suitable scales by varying the spatial resolution (Materka and Strzelecki, 1998).

Most of the wavelet-based image processing methods refer to the two-dimensional wavelet transform (2D-WT). However, 2D-WT treats only planes rather than analyzing multi-spectral bands and, hence, ignores the spectral-spatial correlation. Thus, 3D-WT was introduced for treating cubic data. 3D-WT is a combination of high-pass and low-pass filters, not only in the spatial domain, but also in the spectral direction. However, literature concerning 3D-WT is relatively rare for remote sensing.

Contourlet transform (CT) can effectively deal with images which have smooth contours (Do and Vetterli, 2002). It is based on a two-dimensional non-separable filter bank, which is able to capture the geometrical details of the source image. For CT, a Laplacian pyramid is first used to provide multiscale decomposition, followed by a directional filter bank to provide a directional decomposition.

Texture Fusion for Change Detection

In this study, we propose two strategies for multi-texture change detection: random forests (RF) and a fuzzy set model. The texture change vectors (TCVs), i.e., the differences between the texture feature vectors in bi-temporal images, are calculated for the multi-texture change detection. The processing chain for the proposed framework is shown in Figure 1, and consists of the following three steps:

1. Multitemporal Texture Extraction and Calculation of the TCV.

   After the multitemporal texture extraction, the TCV of each texture is calculated for multi-texture change detection. Please note that, in this research, texture change is used as an indicator of land-cover/use change.

2. Multi-texture Change Detection Based on Random Forests and a Fuzzy Set Model.

   In this study, RF (Breiman, 2001) and a fuzzy set model (Tobias and Rui, 2002; Du *et al.*, 2012) are selected for achieving the multi-texture fusion and change detection.

   RF is a non-parametric machine learning method that can handle a large number of input features (Duro *et al.*, 2012). It can also be used as an embedded method for multi-feature fusion, where the feature selection and learning phases can interact with each other (Tuia *et al.*, 2009). RF is a combination of a series of tree-structured classifiers. For each node of a tree, a bootstrapped sample of the original training samples is randomly selected. The Gini index (Zambon *et al.*, 2006), a standard impurity measure which can avoid variable selection bias, is then used for estimating the importance of each feature. The Gini index is described as:

$$\text{Gini}(m) = 1 - \sum_{i=1}^{L} p_{wi}^{\ 2} \qquad (1)$$

   where L is the number of classes and p_{wi} is the probability or relative frequency of class wi at node m. In this way, it becomes easy to evaluate the performance of different textures in change detection by sorting them in terms of their importance in a descending mANNer. The final results are then obtained by selecting the output of the ensemble of tree classifiers, which is more accurate than using a single classifier alone (Prasad *et al.*, 2006). The RF method is of interest in this research since it is able to simultaneously predict whether or not change takes place in each pixel, and can be used to rank the multiple texture measures.

   On the other hand, with the aim of enhancing the contrast between change and no-change areas, feature fusion based on a fuzzy set model is employed in this research to create the change detection map by combining the multiple TCVs. The fuzzy set model is an unsupervised model that can be used to process a variety of features and implement

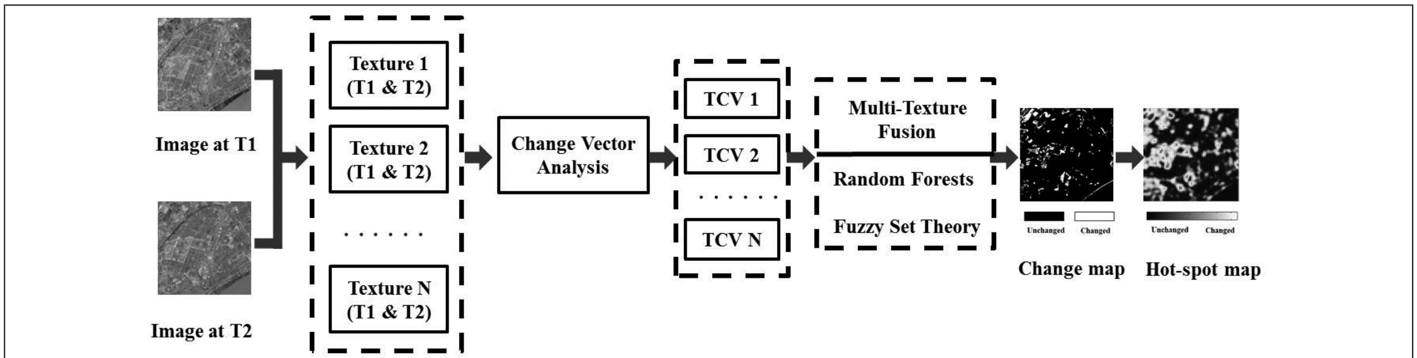

Figure 1. Flowchart of the proposed multi-texture change detection method.

an efficient scheme for multi-feature fusion when little or no prior knowledge is available (Du *et al.*, 2012). Firstly, the *Dc* (degree of change) and *Duc* (degree of no-change) for each pixel in the textural change component of each feature are computed according to the fuzzy membership function. The fusion functions are defined as:

$$Dc(x)=\begin{cases}0, & x \le a \\ 2\{(x-a)/(c-a)\}^2, & a \le x \le b \\ 1-2\{(x-c)/(c-a)\}, & b \le x \le c \\ 1, & x \ge c\end{cases} \tag{2}$$

$$Duc(x)=1-Dc(x) \tag{3}$$

where x is the value of a pixel in the textural change component. The fusion functions are controlled by parameters a and c. In addition, b is given by $b = (a+c)/2$, with $Dc(b)=0.5$, which denotes the crossover point. The final Dc' and Duc' are then calculated as:

$$\begin{Bmatrix} Dc'(x)=\dfrac{1}{N}\sum_{i=1,t\in \mathrm{TEX}}^{N} Dc(x) \\ Duc'(x)=\dfrac{1}{N}\sum_{i=1,t\in \mathrm{TEX}}^{N} Dc(x) \end{Bmatrix} \tag{4}$$

where N is the number of texture features considered. Through the fusion functions, the "probability of change" of each pixel is redefined by the fuzzy set model of texture combinations. Therefore, the inconsistency of the detection performances in the different texture features can be reduced to a great extent (Du *et al.*, 2012; Ahmed *et al.*, 2013). The final results are then obtained by comparing Dc' and Duc':

$$S(x)=\begin{cases} changed, & Dc'(x) \ge Duc'(x) \\ unchanged, & Dc'(x) < Duc'(x)\end{cases} \tag{5}$$

Since individual TCVs contain incomplete target information, the fuzzy set model combining multiple TCVs is able to further improve the accuracy of the detection results.

3. Generation of a Hot-spot Map for Change Analysis

The "hot-spot" detection approach (Pacifici and Del Frate, 2010) is an effective approach for change detection from high-resolution images. In this strategy, the final change map is first divided into a series of patches ($N \times N$ pixels), with an overlap between the adjacent patches of half a patch, which is viewed as the basic unit for change detection. In order to look for "hot spots" where a change is significant, the change density represented by the frequency of changed pixels in each patch is calculated. The change density indicates the potential of a patch being flagged as change, and the patches in light colors represent hot-spot change areas, while the patches with less change appear dark. The processing chain of the generation of a hot-spot map for change analysis is illustrated in Figure 2.

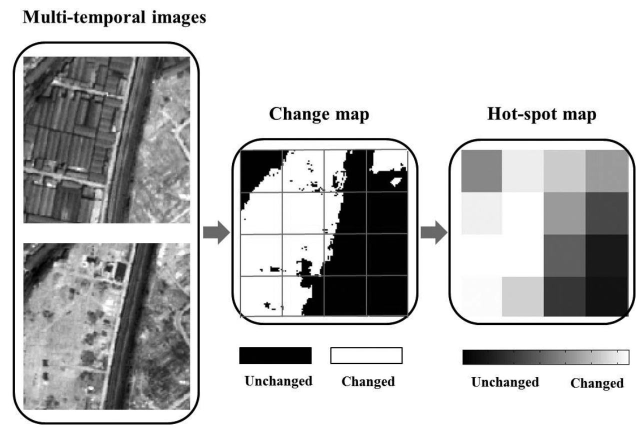

Figure 2. Processing chain of the generation of a hot-spot map for change analysis.

Experiments

Study Site and Datasets

Bi-temporal ZY-3 orthographic images from the city of Wuhan, with the size of 7,500 × 8,000 pixels and a spatial resolution of 2.5 m, were used to compare and validate the performance of the texture-based change detection methods in this research (Figure 3). Wuhan is the capital of Hubei province, which is located in the middle of China. In recent years, this city has experienced an accelerating pace of development. For instance, since the majority of Wuhan's land change is a direct result of the re-plANNing of the old city, a large amount of land-cover change refers to the demolition and construction of buildings. Moreover, development of the infrastructure of this city, such as metro lines, has also been greatly improved. In addition, in order to increase the urban vegetation coverage, a number of public gardens and parks have been constructed, resulting in land-cover change for vegetation.

ZY-3, which was launched on 19 January 2012, is the first civilian high-resolution stereo mapping satellite of China. With an appropriate spatial resolution and geo-location accuracy, ZY-3 can satisfy the needs for various fields, such as mapping, land-use plANNing, agriculture, environmental studies, and urban plANNing. The specifications of the ZY-3 satellite are provided in Table 2. ZY-3 orthographic images were used in this research in order to avoid the effects caused by the geometrical differences between multi-temporal images. Pseudo-invariant features (Schott *et al.*, 1988) were utilized in the relative radiometric correction of multi-temporal remote sensing imagery so that the change characteristics of the geospatial targets could be preserved. The undisturbed water and bare land were selected as pseudo-invariant features. In addition, the two orthographic images were co-registered to a root-mean-square error (RMSE) of less than 1 m.

Experimental Setup

For the transform-based textures, stationary wavelet transform (SWT) (Nason and Silverman, 1995) was adopted to obtain the 2D and 3D wavelet parameters, and the Haar wavelet basis was chosen for its simplicity and robustness. CT was carried out using non-sampled contourlet transform (NSCT) (Cunha *et al.*, 2006) as it is a flexible shift-invariant image analysis method. The Gabor texture features were extracted in four scales, with eight directions for each scale.

With regard to statistical textures, the feature images of GLCM were acquired using four windows (5 × 5, 9 × 9, 13 × 13, and 17 × 17), considering the multiscale characteristics of textures.

The method of box counting (scale parameter = 9) was implemented to estimate the fractal dimension as a representative model-based texture.

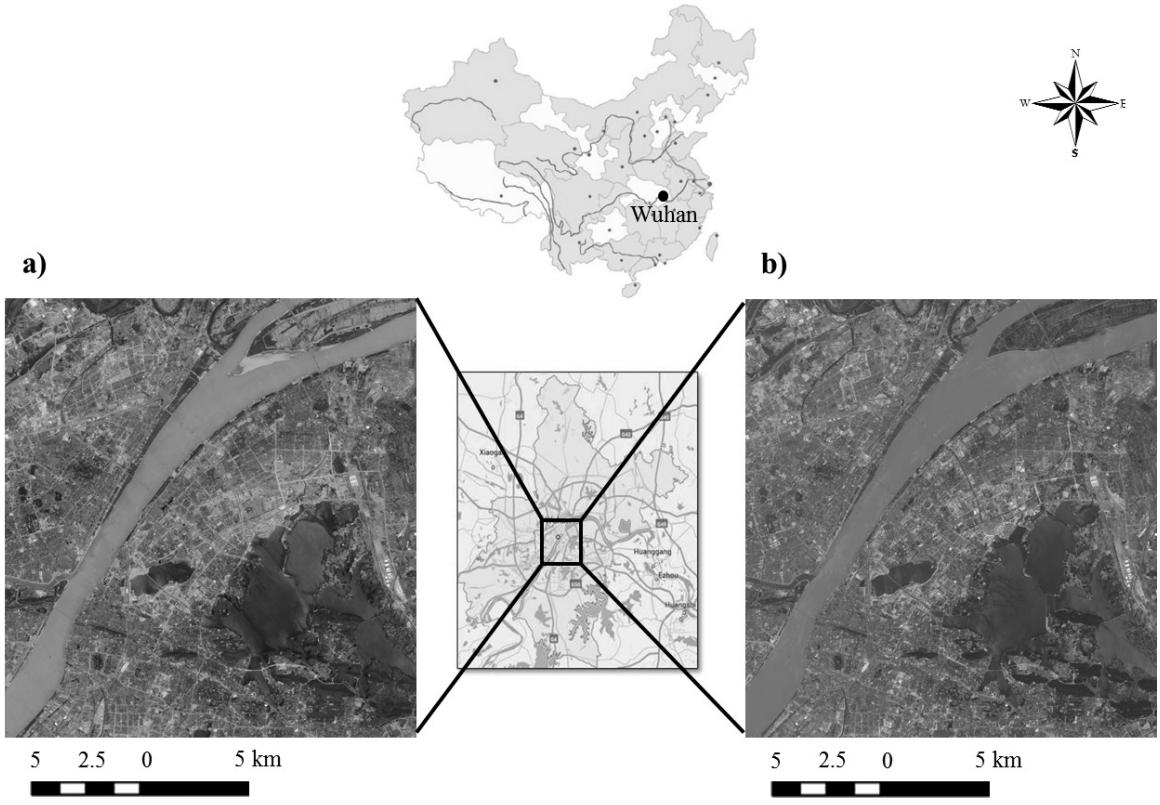

Figure 3. False-color maps of bi-temporal ZY-3 images of the City of Wuhan (Central China), acquired on: (a) 12 June 2012, and (b) 20 August 2013, respectively.

Table 2. The Specifications of the ZY-3 Satellite

Bands	Wavelength	Spatial resolution
Nadir scene panchromatic	500–800 nm	2.1 m
Forward scene panchromatic		3.6 m
Backward scene panchromatic		3.6 m
Blue	450–520 nm	5.8 m
Green	520–590 nm	
Red	630–690 nm	
Infrared	770–890 nm	

MPs, DMPs, and APs are the commonly used morphological textures in the modeling of spatial context information. According to the image resolution, openings and closings by reconstruction, with an SE whose dimension increased from two to six pixels with an increment of two pixels, were used to compute the MPs. A disk-shaped SE allowing a better reconstruction of the borders of the objects was utilized in this research. As for the APs, the attribute of standard deviation, measuring the homogeneity of the regions, was calculated with a series of parameters (10, 40, and 70).

In order to make sure that the change detection results of each texture had a high correctness rate, but a low false alarm rate; the maximum of Youden's index (Youden, 1950) was used to estimate the optimal threshold T for each texture, in terms of the receiver operating characteristic (ROC) curves (Fawcett, 2006). The ROC curves are parametric curves plotting true positive rate (TPR) (vertical axis) against false positive rate (FPR) (horizontal axis), and they are calculated for all possible thresholds. The point that is closest to the upper left corner in a ROC curve is assumed to be the optimal threshold value, corresponding to a high correctness rate but a low false alarm rate. The parameters a and c of the fuzzy set fusion were set to $0.8T$ and T, respectively.

The ground reference map, showing the changed and unchanged areas in the study area, was carefully produced by manual photointerpretation based on our rich prior knowledge and a series of exhaustive field campaigns in the city of Wuhan. The ground reference includes 1,258,442 changed pixels. Four indexes were used to evaluate the accuracy of the change detection by comparing the detection results and the ground reference map: 1) correctness; 2) omission errors (Congalton and Green, 1999); 3) commission errors (Congalton and Green, 1999); and 4) overall errors.

$$Correctness = \frac{TP}{TP + FN} \tag{6}$$

$$Omission\ errors = \frac{FN}{TP = FN} \tag{7}$$

$$Commission\ errors = \frac{FP}{TP + FP} \tag{8}$$

$$Overall\ errors = \frac{2 * Commission\ errors * Omission\ errors}{Commission\ errors + Omission\ errors} \tag{9}$$

$$Commission\ errors + Omission\ errors$$

where TP is the number of correctly detected changed pixels and FN is the number of missed changed pixels. FP and TN are the numbers of unchanged pixels in the ground reference, but detected as changed and unchanged in the result, respectively.

The overall errors defined in this paper indicate a balance between omission and commission errors.

Results of the Spectral-Textural Features for Change Detection

The results for the spectral bands combined with the ten selected texture features are presented in Table 3. The first comment with regard to the table is that 2D-WT, 3D-WT, and the APs achieve the best results in terms of their high correctness and low overall error, compared to the other texture features. The statistical textures do not produce satisfactory results in this study. With regard to the fractal model, its accuracy is comparable to or even better than some of the other texture features, such as the PSI texture. However, the accuracy of the fractal method is lower than the accuracy of the WT-based textures and the APs.

Table 3. Accuracy of the Spectral-textural Change Detection (ZY-3 Imagery of Wuhan, Central China)

Category of texture	Methods	Correctness (%)	OE (%)	CE (%)	Overall errors (%)
Statistical texture	Spe + GLCM	73.83	26.17	6.02	9.79
	Spe + PSI	70.18	29.82	5.69	9.56
Structural texture	Spe + MPs	72.49	27.51	5.47	9.13
	Spe + DMPs	74.79	25.21	6.00	10.01
	Spe + APs	83.53	16.47	5.98	8.74
Transform-based texture	Spe + Wavelet 2D	82.98	17.02	5.58	8.40
	Spe + Wavelet 3D	84.41	15.59	5.92	8.58
	Spe + Gabor	72.81	27.19	6.04	9.88
	Spe + Contourlet	76.41	23.59	5.99	9.55
Model-based texture	Spe + Fractal	74.47	25.53	5.93	9.62

Results of the Multi-Texture Change Detection

Considering that a mono-texture is not sufficient to describe complex and varied geospatial targets, we propose to exploit multi-texture fusion strategies for change detection. The accuracy indexes for the proposed multi-texture change detection are shown in Table 4, allowing the following observations:

1. Although the change detection results of the mono-texture differ in the commission or omission errors, the multi-texture fusion strategies have the potential to obtain better performance.
2. In the RF-based multi-texture change detection, the results indicate that the combination of the local texture descriptor, morphological APs, and the macro-texture wavelet transform (2D-WT and 3D-WT) achieves the most accurate change detection result (the highest correctness and the lowest error).
3. The performance of the fuzzy set model are similar to RF. Once again, the highest accuracy for the multi-texture change detection is obtained by combining the APs and WT (2D-WT and 3D-WT). This phenomenon shows that in the case presented in this study, the combination of the optimal local and macro-texture features is the most appropriate way to perform multi-texture change detection. It is interesting to note that using all the texture features gives the worst result. This can be partly attributed to the fact that the fuzzy set model aims to reduce the inconsistency of the detection performances of the different TCVs and, hence, including all the textures in the fuzzy set model can instead lead to lower correctness.

Visual Inspection

In order to better understand the performance of the various textures for change detection, some of the change intensity maps, as well as their results, are shown and compared in Figure 4.

The example in Figure 4 shows a typical urban change in Wuhan, where a lot of buildings have been removed due to the city re-plANNing. Please note that the change intensity for each texture feature is represented by the TCV, and the binary result was generated with a threshold chosen according to Youden's index. From the figure, it can be seen that APs and wavelet textures perform better than GLCM and the fractal method, as they show a more complete response for the changed areas. It is interesting to see that the APs can better preserve the shape and contours of the change areas, indicating that APs are an effective local texture descriptor, whereas the wavelet texture is capable of delineating the entire change area and reducing the omission errors. The fractal texture can also preserve the shape and contours of the changed areas, but it leads to a number of omission errors.

The last row in Figure 4 shows the multi-texture fusion results for change detection, where it can be clearly seen that the changed areas are detected more accurately by the fusion methods than the individual methods. RF and the fuzzy fusion of texture combination (APs+2D-WT+3D-WT) give similar results, achieving a better tradeoff between correctness and false alarm rate. The results of RF and the fuzzy fusion of all textures are shown for comparison.

Another example is presented in Figure 5. This case is also related to urban renewal, including a series of land-cover transitions, e.g., from bare land to buildings, and from vegetation and old buildings to bare land (for construction). From the figures, it can be seen that the APs and wavelet methods focus on detailed and macro-textures, respectively. The GLCM texture in this example also shows a satisfactory performance, but it is subject to false alarms. With respect to the multi-texture fusion, RF and the fuzzy set model with the texture combination (APs+2D-WT+3D-WT) yield the best visual results, producing a high correctness rate and small omission and commission errors.

Results of the Urban Hot-Spot Change Analysis

In this subsection, the use of the multi-texture change detection method for urban change analysis is analyzed using

Table 4. Accuracy Assessment of the Proposed Multi-texture Change Detection Method (ZY-3 Imagery of Wuhan, Central China)

Method	Texture combination	Correctness (%)	OE (%)	CE (%)	Overall errors (%)
Random forest	APs+2D-WT	85.92	14.08	5.61	8.02
	APs+2D-WT+3D-WT	86.95	13.05	5.33	7.56
	APs+2D-WT+3D-WT+GLCM	84.07	15.93	5.42	8.08
	APs+2D-WT+3D-WT+Fractal	84.16	15.84	5.40	8.05
	ALL textures	83.88	16.12	5.49	8.19
Fuzzy set	APs+2D-WT	85.03	14.97	5.58	8.13
	APs+2D WT+3D-WT	86.58	13.42	5.46	7.79
	APs+2D-WT+3D-WT+GLCM	83.25	16.75	5.41	8.18
	APs+2D-WT+3D-WT+Fractal	83.91	16.09	5.37	8.07
	ALL textures	82.31	17.69	5.36	8.22

imagery from the center of the City of Wuhan. The size of each patch is 64 × 64 pixels. Figure 6 illustrates the change intensity map obtained by the RF-based texture combination (APs+2D-WT+3D-WT). The patches in red represent the hot-spot change areas, while the patches with less change are in dark blue.

If the change intensity of a unit (e.g., a patch) is larger than a threshold, it is identified as a "salient" change. To evaluate the hot-spot change maps in a more targeted mANNer, we collected all the salient changed patches representing change regions in the hot-spot change maps. Each patch was reevaluated by manual photointerpretation to determine the correctness, and we labeled the change types and cases accordingly. Among the 99 salient changed patches in the hot-spot change maps, 94 patches were correctly detected. Several salient patches in the hot-spot change maps were selected for further analysis in Figure 7 and Table 5.

Discussion

This section consists of three parts. The first part describes the comparison between the textural- and spectral-based methods. Next, two additional datasets are introduced to test the performance and characteristics of the different textures for change detection. Finally, the importance of the different texture features is investigated.

Comparison Between the Textural-Based and Spectral-based Methods

Table 6 lists the results of the spectral-only and textural-only change detection methods. Compared with the spectral-only change detection, some texture-based methods, such as the WT-based textures and the APs, show much more accurate results due to their ability to represent image features in the spatial domain. This indicates that the spatial completeness and consistency of the change information can be acquired by these texture features. Other textural measures, e.g., the GLCM and the Gabor texture feature, achieve comparable accuracies to the spectral-based method for change detection.

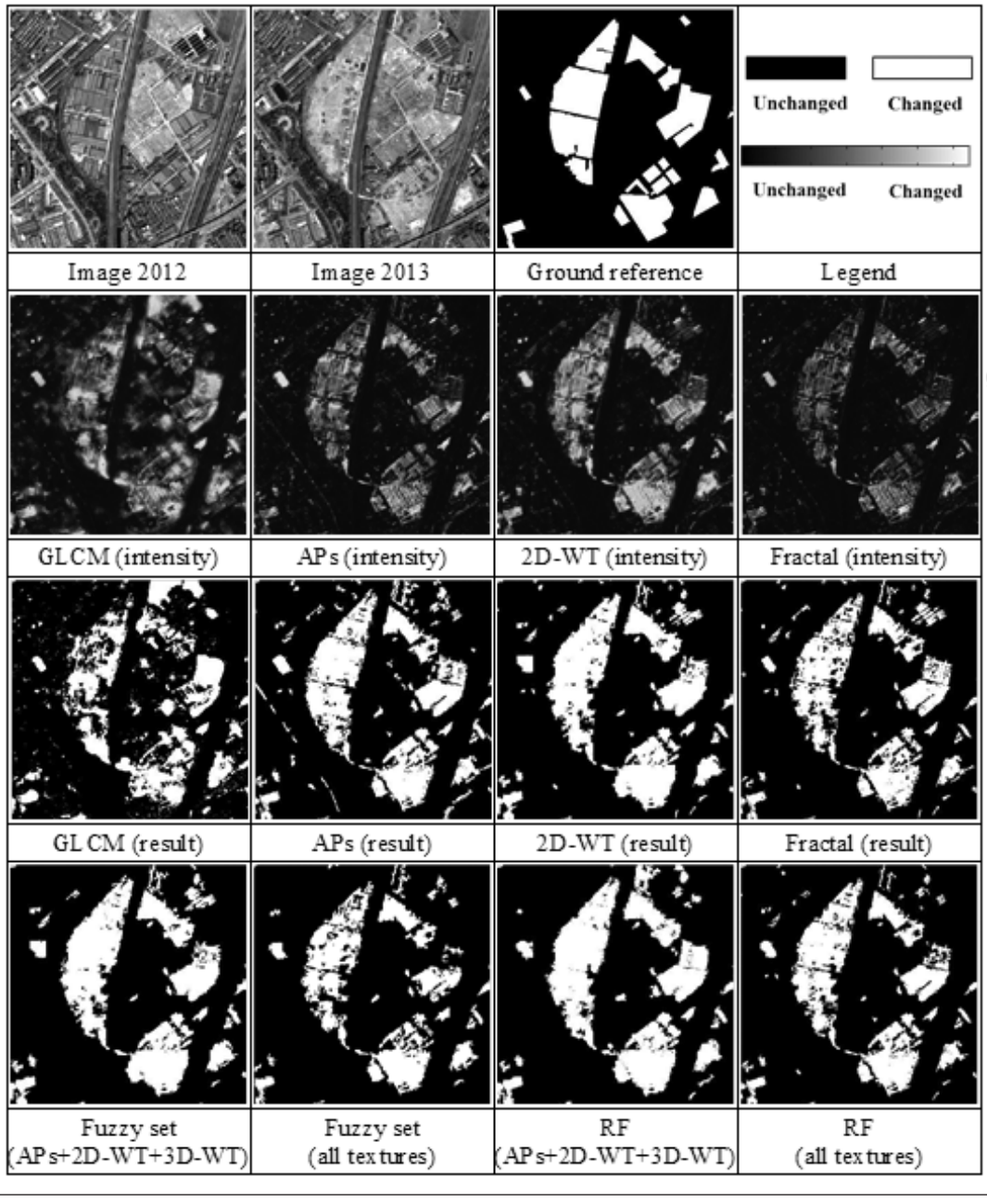

Figure 4. Example showing the change intensity and the results of the change detection (ZY-3 imagery of Wuhan, Central China).

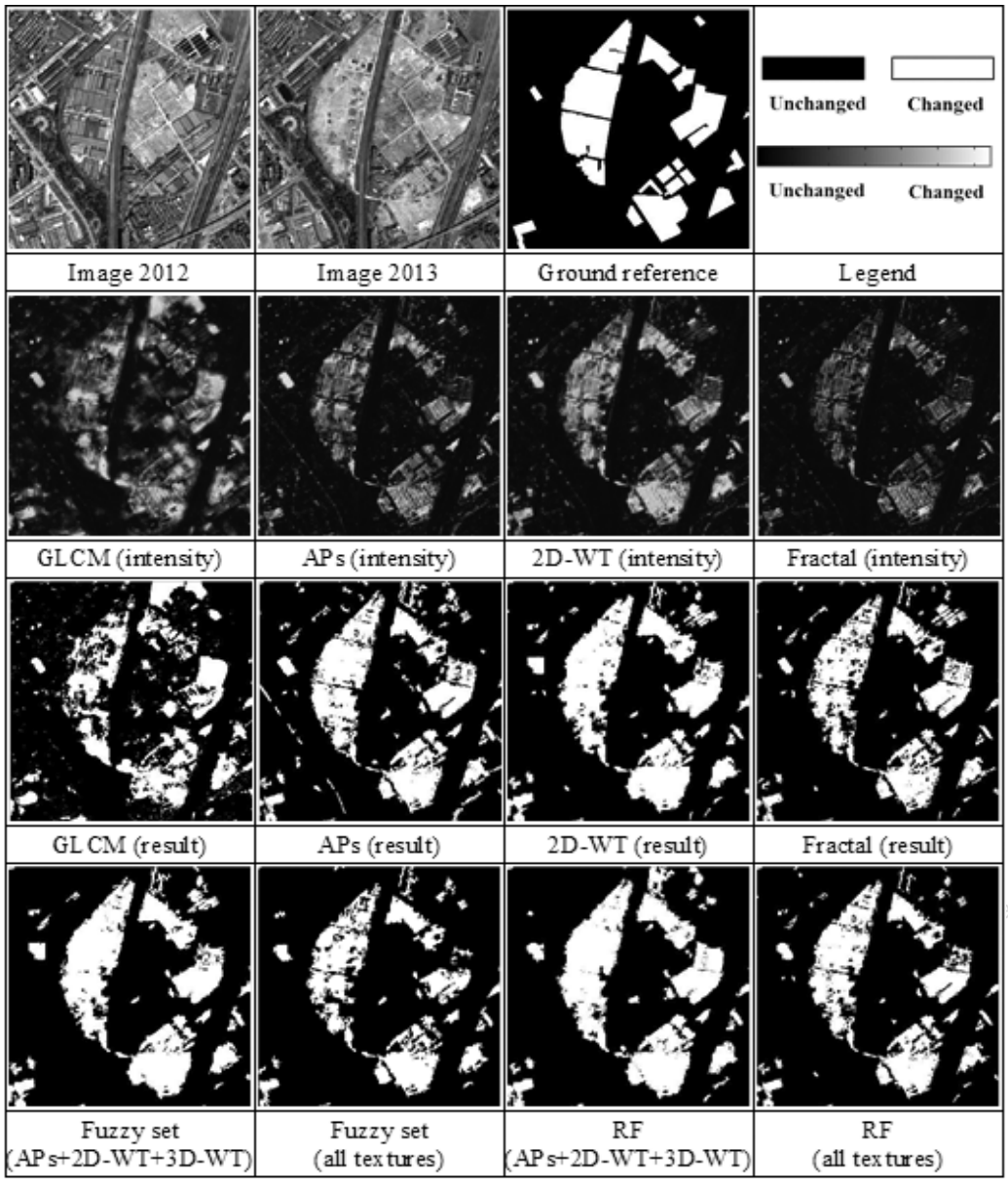

Figure 5. Second example showing the change intensity and the results of the change detection (ZY-3 imagery of Wuhan, Central China)

Additional Datasets

Another two datasets, ZY-3 multi-temporal images (with the size of 6,855 × 7,323 pixels and a spatial resolution of 2.5 m) of the City of Tokyo (the capital of Japan) and WorldView-2 multitemporal images (with the size of 2,902 × 3,313 pixels and a spatial resolution of 2 m) of the City of Kuala Lumpur (the capital of Malaysia), were used to test the performance and characteristics of the different textures for change detection. The bi-temporal images and final change maps of the RF-based texture combination (APs+2D WT+3D WT) are provided in Figure 8.

The additional datasets show similar results and trends. For example, it can be seen that the wavelet-based features obtain the highest accuracy among the macro-textures, while the morphological attributes obtain the best results for the micro-textures (Table 7). Moreover, it can be seen that the RF texture combination (APs + 2D-WT + 3D-WT) also achieves a better tradeoff between commission and omission errors (Table 8). This result means that urban features can be effectively captured by the combination of the optimal local and macro-texture features. Therefore, integrating both micro- and

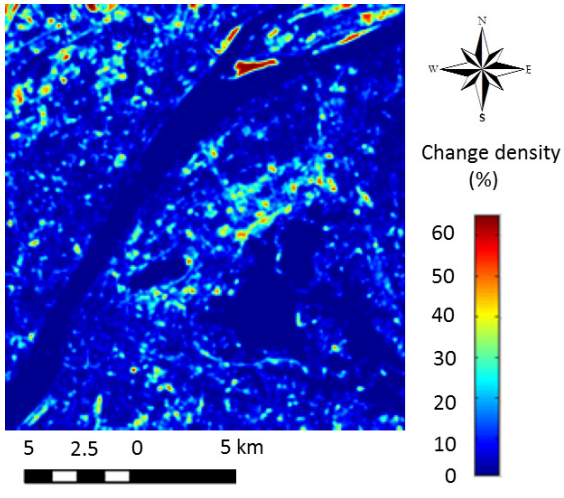

Figure 6. The change map of the RF-based texture combination (APs+2D-WT+3D-WT).

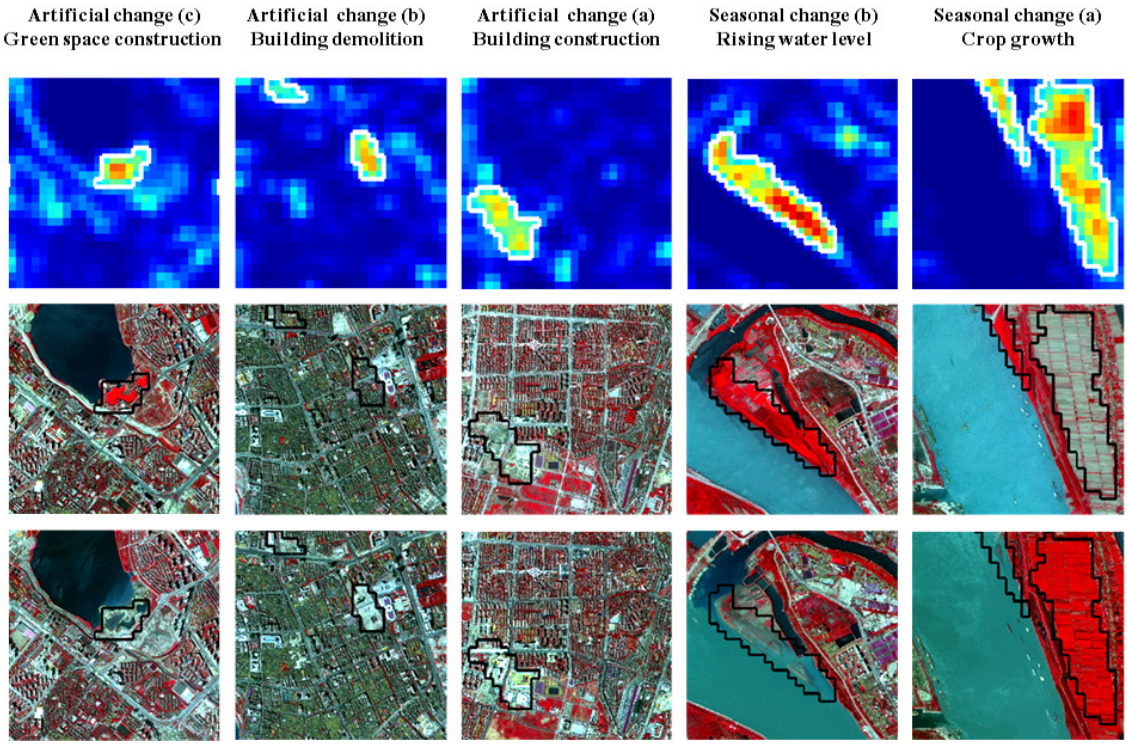

Figure 7. Several examples of changed patches.

Table 5. Analysis of Representative Examples of Changed Patches

Change Types	Cases	Description
Seasonal change	(a) Crop growth	Due to the seasonal effects of crops, bare land turned into farmland.
	(b) Rising water level	Vegetation disappeared due to the rising water level caused by flooding.
Artificial change	(a) Building construction	As a result of building construction, bare land changed into construction sites.
	(b) Building demolition	This was a typical example of renewal of old city areas, where old residential buildings werre demolished.
	(c) Green space construction	Owing to the construction of a new garden from 2012 to 2013, a large number of aquatic plants and terrestrial plants were grown, leading to a significantly increased green coverage.

Table 6. Accuracy of Spectral-only and Textural-only Change Detection (ZY-3 Imagery Of Wuhan, Central China)

Change detection	Category of texture	Methods	Correctness (%)	OE (%)	CE (%)	Overall errors (%)
Textural only	Statistical texture	GLCM	70.54	29.46	6.35	10.45
		PSI	70.01	29.99	5.96	9.94
	Structural texture	MPs	70.32	29.68	5.76	9.65
		DMPs	71.48	28.52	6.30	10.32
		APs	80.83	19.17	6.29	**9.47**
	Transform-based texture	2D-WT	80.41	19.52	5.84	**8.99**
		3D-WT	81.21	18.79	6.24	**9.37**
		Gabor	70.39	29.61	6.37	10.48
		Contourlet	73.25	26.75	6.32	10.22
	Model-based texture	Fractal	71.17	28.83	6.21	10.23
Spectral only			70.16	29.84	6.19	10.25

macro-textures is an appropriate way to perform multi-texture change detection in the selected test datasets.

Investigation of the Importance of the Different Texture Features

The relative importance or weighting of the different texture features is shown in Figure 9. It can be seen that the accuracy trends (Table 3 and Table 8) and the feature importance (Figure 9) are consistent in the three test datasets: 2D-WT and 3D-WT show the highest importance scores among the macro-textures, and the AP textures have the most significant weight among the local texture descriptors.

In this research, the wavelet-based textures obtain the best change detection results in the three datasets. On the one hand, 2D-WT and 3D-WT can provide a macro-textural

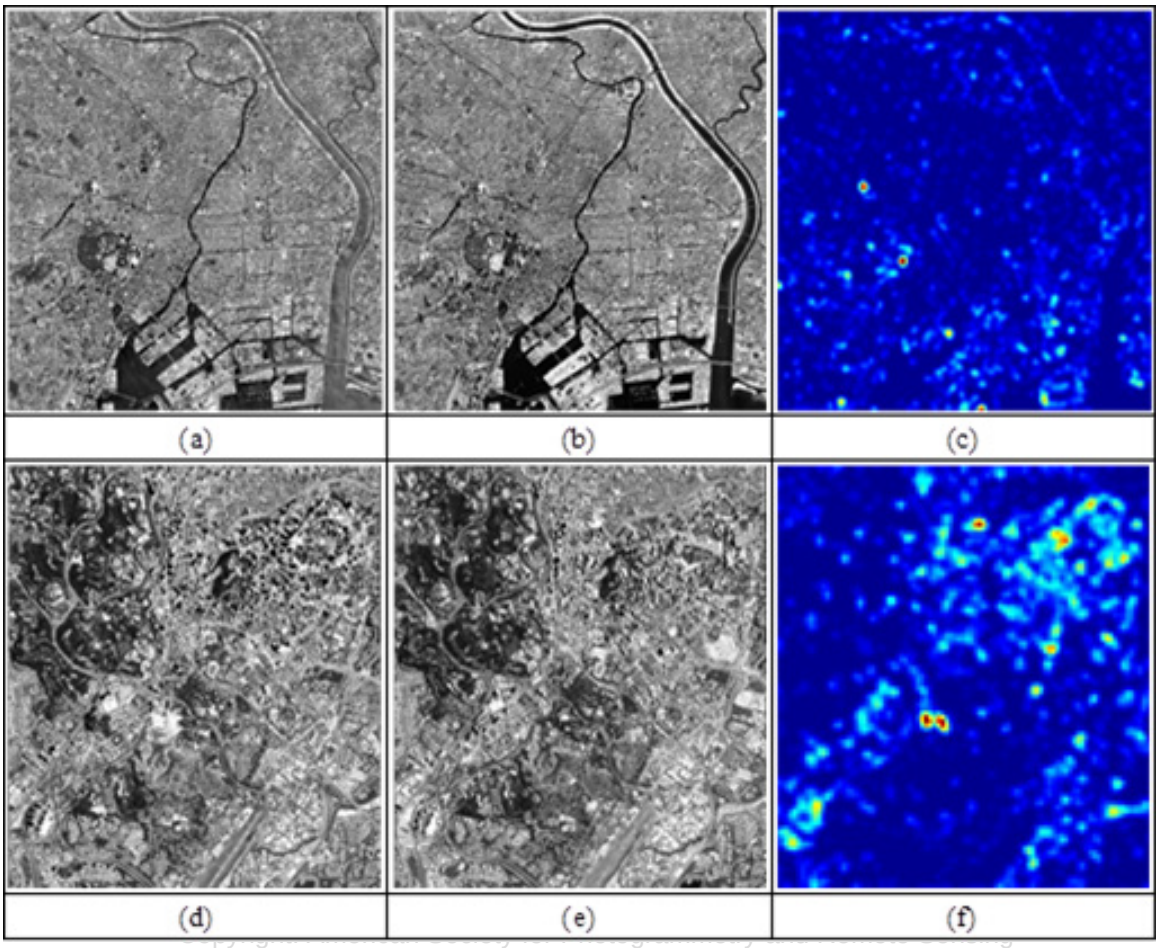

Figure 8. False-color maps of bi-temporal ZY-3 images of the City of Tokyo, acquired on (a) 31 March 2014, and (b) 04 February 2015, respectively, as well as (c) the change map. False-color maps of bi-temporal WorldView-2 images of the City of Kuala Lumpur, acquired on (d) 17 February 2011, and (e) 27 June 2014, respectively, as well as (f) the change map.

Table 7. Accuracy of the Spectral-textural Change Detection

Dataset	Category of texture	Method	Correctness (%)	OE (%)	CE (%)	Overall errors (%)
ZY-3 images of the City of Tokyo	Statistical textures	Spe + GLCM	77.82	22.18	6.37	9.90
		Spe + PSI	72.87	27.13	5.85	9.62
	Structural textures	Spe + MPs	73.98	26.02	5.82	9.51
		Spe + DMPs	74.76	25.24	6.01	9.71
		Spe + APs	82.97	17.03	6.03	**8.91**
	Transform-based textures	Spe + 2D-WT	83.84	16.16	5.84	**8.58**
		Spe + 3D-WT	84.35	15.65	6.02	**8.70**
		Spe + Gabor	73.53	26.47	6.12	9.94
		Spe + Contourlet	72.29	27.71	6.09	9.96
	Model-based texture	Spe + Fractal	71.61	28.39	5.97	9.87
WorldView-2 images of the City of Kuala Lumpur	Statistical textures	Spe + GLCM	76.67	23.33	6.41	10.06
		Spe + PSI	72.05	27.95	5.76	9.55
	Structural textures	Spe + MPs	73.67	26.33	5.63	9.28
		Spe + DMPs	73.41	26.59	6.09	9.91
		Spe + APs	83.82	16.12	6.05	**8.80**
	Transform-based textures	Spe + 2D-WT	84.03	15.97	5.79	**8.50**
		Spe + 3D-WT	83.46	16.54	6.07	**8.88**
		Spe + Gabor	72.14	27.86	6.18	10.12
		Spe + Contourlet	72.85	27.15	6.14	10.02
	Model-based textures	Spe + Fractal	71.08	28.92	6.02	9.97

description with multi-resolution spectral and spatial information (Ouma and Tateishi, 2008). On the other hand, the WT-based textures are able to obtain an accurate interpretation of multidirectional or omni-directional textural primitives (Ouma *et al.*, 2008). When compared with the results of the other transform-based textures, such as the Gabor texture feature, the WT-based textures appear to be more valuable for the detection of changed areas. Such a result can be potentially explained by the fact that they can provide a unified framework with reduced inter-scale correlation among the resulting texture components (Ouma *et al.*, 2010). 3D WT, which is exploited here in change detection and analysis for the first time, is a satisfactory method for change detection when compared to the other state-of-the-art methods. In addition, among the local textures, the change information in the scene is well extracted and characterized by the APs. This result is consistent with the findings of other researchers (Falco *et al.*, 2013; Dalla Mura *et al.*, 2010), indicating the effectiveness of the APs in modeling spatial context information by exploiting local attributes (e.g., area, moment of inertia, standard deviation).

The GLCM texture, which has been widely used in the existing literature to extract spatial information from very high resolution urban scenes, also shows a relatively high importance score. This can be interpreted as follows. In urban areas, shadows may offer additional geometric and semantic information on the shape and orientation of the geographic targets (Pacifici *et al.*, 2009). The difference in the homogeneity (the selected GLCM texture in this research) between shadowed buildings and non-shadowed buildings is beneficial to the discrimination of such changes (Pacifici *et al.*, 2009). However, the fractal method shows a lower importance score than the other texture features, as it does not utilize the texture property sufficiently in change detection, i.e., different geospatial targets may have the same fraction value. The above interpretations also fit well with the visual inspection of the change detection results presented in the Visible Inspection Section.

When applied to different data and areas, 2D-WT, 3D-WT, and the APs also exhibit a relatively high importance score when compared to the other texture features. This shows the potential of such features for extracting the characteristics and local details in a scene. Consequently, it is reasonable to assume that their combination, i.e., in a multi-texture fusion mANNer, can lead to a better performance. As the texture analysis in this study was carried out with data from three different cities, we believe that this investigation could be efficiently extended to new scenes.

Conclusions

In this paper, a number of representative texture measures were selected to detect change from multi-temporal remote sensing images. Subsequently, characteristics of the selected mono-texture were evaluated by a comparison of their change detection results. Based on the observation that a single texture feature is not sufficient to describe complex geospatial image scenes, we integrated the local and macro-textures to further enhance the performance of change detection.

The effectiveness of the selected mono-texture and the proposed fusion strategies were validated on ZY-3 orthographic images of the City of Wuhan (Central China) and the City of Tokyo (the capital of Japan), as well as WorldView-2 multispectral images of the City of Kuala Lumpur (the capital of Malaysia). The following conclusions can be drawn:

1. Compared with the spectral-based methods, the texture-based change detection methods can obtain more accurate results due to their better ability to represent image features in the spatial domain.

Table 8. Accuracy Assessment of the Multi-texture Change Detection Methods

Dataset	Method	Texture combination	Correctness (%)	OE (%)	CE (%)	Overall errors (%)
ZY-3 images of the City of Tokyo	Random forest	APs+2D-WT	85.95	14.05	5.61	8.02
		APs+2D-WT+3D-WT	87.01	12.99	5.28	7.51
		APs+2D-WT+3D-WT+GLCM	85.03	14.97	5.51	8.06
		APs+2D-WT+3D-WT+Fractal	84.52	15.48	5.42	8.03
		ALL textures	83.34	16.66	5.48	8.25
WorldView-2 images of the City of Kuala Lumpur	Random forest	APs+2D-WT	85.41	14.59	5.58	8.07
		APs+2D-WT+3D-WT	86.68	13.32	5.31	7.58
		APs+2D-WT+3D-WT+GLCM	84.52	15.48	5.47	8.08
		APs+2D-WT+3D-WT+Fractal	84.09	15.92	5.36	8.02
		ALL textures	82.96	17.04	5.43	8.24

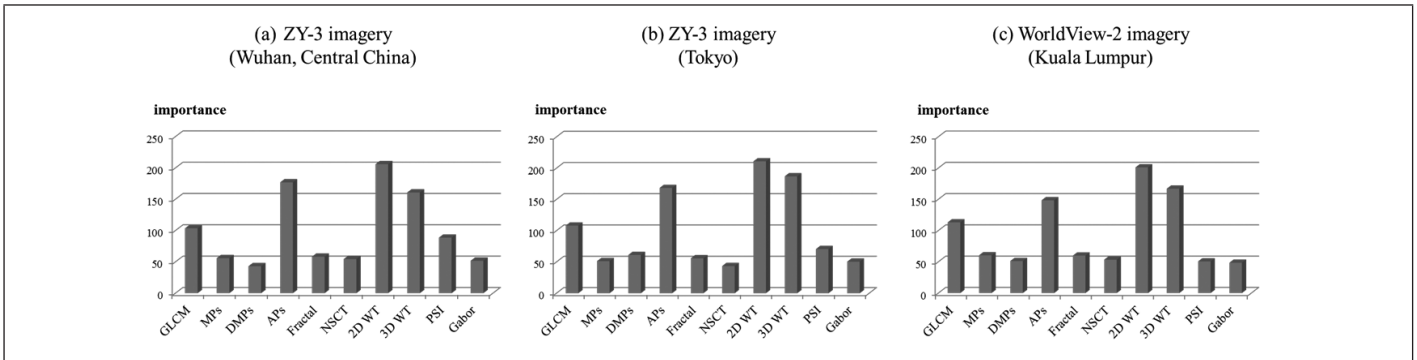

Figure 9. Importance of the texture features extracted from the ZY-3 imagery of the City of Wuhan (a) and the City of Tokyo (b), as well as WorldView-2 imagery of the City of Kuala Lumpur (c).

2. Following the analysis of the performance of the mono-texture in change detection, it was found that two-dimensional wavelet transform (2D-WT), three-dimensional wavelet transform (3D-WT), and attribute profiles (APs) can achieve better results than the other textures. Furthermore, it was found that the WT-based and APs-based textures are effective in describing the macro- and micro-structures in change detection, respectively, corresponding to the whole characteristics and local details.
3. 3D-WT, which was exploited here in change detection and analysis for the first time, was found to be a satisfactory method for change detection when compared to the other state-of-the-art methods.
4. Considering that a mono-texture is not able to sufficiently describe complex urban scenes, we proposed a multi-texture change detection method integrating both micro- and macro-texture. The experimental results showed that texture combination (wavelet-based macro-textures and the morphological attribute-based local texture) by both random forests (RF) and a fuzzy set model can further improve the accuracy of texture-based change detection.
5. The proposed multi-texture fusion method for change detection, which was used to accurately detect seasonal and artificial change in urban areas, will be of practical value for the monitoring of fast-growing urban areas. The proposed method has the potential to become a routine strategy for urban monitoring and plANNing. However, one limitation of the proposed method is that it cANNot provide the specific change types, which will be the focus of our future work (Ye and Chen, 2015).

Acknowledgments

The work presented in this paper was supported in part by the National Key Research and Development Program of China under Grant 2016YFB0501403, in part by China Science Fund for Excellent Young Scholars under Grant 41522110, and in part by the Foundation for the Author of National Excellent Doctoral Dissertation of PR China (FANEDD) under Grant 201348. The authors would like to thank the anonymous reviewers for their insightful and constructive comments, which significantly improved the quality of this paper.

References

Aghababaee, H., Y.C. Tzeng, and J. Amini, 2012. Swarm intelligence and fractals in dual-pol synthetic aperture radar image change detection, *Journal of Applied Remote Sensing*, 6(16):197–205.

Ahmed, B., R. Ahmed, and X. Zhu, 2013. Evaluation of model validation techniques in land cover dynamics, *ISPRS International Journal of Geo-Information*, 2(3):577–597.

Al-Khudhairy, D.H.A., 2005. Structural damage assessments from Ikonos data using change detection, object-oriented segmentation, and classification techniques, *Photogrammetric Engineering & Remote Sensing*, 71(7):825–838.

Breiman, L., 2001. Random forests, *Machine Learning*, 45(1):5–32.

Carleer, A.P., and E. Wolff, 2006. Urban land cover multi-level region-based classification of VHR data by selecting relevant features, *International Journal of Remote Sensing*, 27(6):1035–1051.

Chen, J., P. Gong, C. He, R. Pu, and P. Shi, 2003. Land-use/land-cover change detection using improved change-vector analysis, *Photogrammetric Engineering & Remote Sensing*, 69(4):369–379.

Clarke, K.C., 1986. Computation of the fractal dimension of topographic surfaces using the triangular prism surface area method, *Computers & Geosciences*, 12(5):713–722.

Congalton, R.G., and K. Green, 1999. *Assessing the Accuracy of Remotely Sensed Data: Principles and practices*, CRC/Lewis Press, Boca Raton, Florida, 137 p.

Cunha, A.L.Da., Z. Jianping, and M.N. Do, 2006. The nonsubsampled contourlet transform: Theory, design, and applications, *IEEE Transactions on Image Processing*, 15(10):3089–3101.

Dalla Mura, M., J.A. Benediktsson, F. Bovolo, and L. Bruzzone, 2008. An unsupervised technique based on morphological filters for change detection in very high resolution images, *IEEE Geoscience and Remote Sensing Letters*, 5(3):433–437.

Dalla Mura, M., J.A. Benediktsson, B. Waske, and L. Bruzzone, 2010. Morphological attribute profiles for the analysis of very high resolution images, *IEEE Transactions on Geoscience and Remote Sensing*, 48(10):3747–3762.

Daugman, J.G., 1975. Uncertainty relation for resolution in space, spatial frequency, and orientation optimized by two-dimensional cortical filters, *Journal of the Optical Society of America*, 2(7):1160–1169.

Do, M.N., and M. Vetterli, 2002. Contourlet: A directional multiresolution image representation, *Proceedings of IEEE ICIP*, 1:I-357–I-360.

Du, P., S. Liu, P. Gamba, K. Tan, and J. Xia, 2012. Fusion of difference images for change detection over urban areas, *IEEE Journal of Selected Topics in Applied Earth Observations and Remote Sensing*, 5(4):1076–1086.

Duro, D.C., S.E. Franklin, and M.G. Dubé, 2012. Multi-scale object-based image analysis and feature selection of multi-sensor earth observation imagery using random forests, *International Journal of Remote Sensing*, 33(14):4502–4526.

Falco, N., M.D. Mura, F. Bovolo, J.A. Benediktsson, and L. Bruzzone, 2013. Change detection in VHR images based on morphological attribute profiles, *IEEE Geoscience and Remote Sensing Letters*, 10(3):636–640.

Fawcett, T., 2006. An introduction to ROC analysis, *Pattern Recognition Letters*, 27(8):861–874.

Ghamisi, P., M. Dalla Mura, and J.A. Benediktsson, 2015. A survey on spectral and spatial classification techniques based on attribute profiles, *IEEE Transactions on Geoscience and Remote Sensing*, 53(5):2335–2353.

Goodchild, M.F., 1980. Fractals and the accuracy of geographical measures, *Journal of the International Association for Mathematical Geology*, 12(2):85–98.

Haralick, R.M., K. Shanmugam, and I.H. Dinstein, 1973. Textural features for image classification, *IEEE Transactions on Systems, Man, and Cybernetics*, SMC-3(6):610–621.

He, C., A. Wei, P. Shi, Q. Zhang, and Y. Zhao, 2011. Detecting land-use/land-cover change in rural-urban fringe areas using extended change-vector analysis, *International Journal of Applied Earth Observation and Geoinformation*, 13(4):572–585.

Homer, C., J. Dewitz, L. Yang, S. Jin, P. Danielson, G. Xian, J. Coulston, N. Herold, J. Wickham, and K. Megown, 2015. Completion of the 2011 National Land Cover Database for the conterminous United States - Representing a decade of land cover change information, *Photogrammetric Engineering & Remote Sensing*, 81(5):346–354.

Huang, S., X. Cai, S. Chen, and D. Liu, 2011. Change detection method based on fractal model and wavelet transform for multitemporal SAR images, *International Journal of Applied Earth Observation and Geoinformation*, 13(6):863–872.

Huang, X., and L. Zhang, 2012. Morphological building/shadow index for building extraction from high-resolution imagery over urban areas, *IEEE Journal of Selected Topics in Applied Earth Observations and Remote Sensing*, 5(1):161–172.

Huang, X., and L. Zhang, 2013. An SVM ensemble approach combining spectral, structural, and semantic features for the classification of high-resolution remotely sensed imagery, *IEEE Transactions on Geoscience and Remote Sensing*, 51(1):257–272.

Huang, X., L. Zhang, and P. Li, 2007. Classification and extraction of spatial features in urban areas using high-resolution multispectral imagery, *IEEE Geoscience and Remote Sensing Letters*, 4(2):260–264.

Im, J., Z. Lu, and J.R. Jensen, 2011. A genetic algorithm approach to moving threshold optimization for binary change detection, *Photogrammetric Engineering & Remote Sensing*, 77(2):167–180.

Johansen, K., L.A. Arroyo, S. Phinn, C. Witte, G.J. Hay, and T. Blaschke, 2010. Comparison of geo-object based and pixel-based change detection of riparian environments using high spatial resolution multi-spectral imagery, *Photogrammetric Engineering & Remote Sensing*, 76(2):123–136.

Keller, J.M., S. Chen, and R.M. Crownover, 1989. Texture description and segmentation through fractal geometry, *Computer Vision, Graphics, and Image Processing*, 45(2):150–166.

Kit, O., and M. Lüdeke, 2013. Automated detection of slum area change in Hyderabad, India using multitemporal satellite imagery, *ISPRS Journal of Photogrammetry and Remote Sensing*, 83:130–137.

Klonus, S., D. Tomowski, M. Ehlers, P. Reinartz, and U. Michel, 2012. Combined edge segment texture analysis for the detection of damaged buildings in crisis areas, *IEEE Journal of Selected Topics in Applied Earth Observations and Remote Sensing*, 5(4):1118–1128.

Li, W., K. Sun, and H. Zhang, 2014. Algorithm for relative radiometric consistency process of remote sensing images based on object-oriented smoothing and contourlet transforms, *Journal of Applied Remote Sensing*, 8(7):4480–4494.

Liu, X., and R.G. Lathrop Jr., 2002. Urban change detection based on an artificial neural network, *International Journal of Remote Sensing*, 23(12):2513–2518.

Mallat, S.G., 1989. Multifrequency channel decompositions of images and wavelet models, *IEEE Transactions on Acoustics Speech and Signal Processing*, 37(12):2091–2110.

Mandelbrot, B.B., 1983. *The Fractal Geometry of Nature*, revised and enlarged edition, W.H. Freeman & Co., New York.

Materka, A., and M. Strzelecki, 1998. Texture analysis methods - A review, Technical University of Lodz, Institute of Electronics, *COST B11 Report*, Brussels, pp. 9–11.

Nason, G.P., and B.W. Silverman, 1995. The stationary wavelet transform and some statistical applications, *Lecture Notes in Statistics*, 103:281–300.

Ouma, Y.O., J. Tetuko, and R. Tateishi, 2008. Analysis of co-occurrence and discrete wavelet transform textures for differentiation of forest and non-forest vegetation in very-high-resolution optical-sensor imagery, *International Journal of Remote Sensing*, 29(12):3417–3456.

Ouma, Y.O., and R. Tateishi, 2008. Urban-trees extraction from QuickBird imagery using multiscale Spectex filtering and non-parametric classification, *ISPRS Journal of Photogrammetry and Remote Sensing*, 63(3):333–351.

Ouma, Y.O., R. Tateishi, and J.T. Sri-Sumantyo, 2010. Urban features recognition and extraction from very-high resolution multi-spectral satellite imagery: A micro-macro texture determination and integration framework, *IET Image Processing*, 4(4):235–254.

Pacifici, F., and F. Del Frate, 2010. Automatic change detection in very high resolution images with pulse-coupled neural networks, *IEEE Geoscience and Remote Sensing Letters*, 7(1):58–62.

Pacifici, F., M. Chini, and W.J. Emery, 2009. A neural network approach using multi-scale textural metrics from very high-resolution panchromatic imagery for urban land-use classification, *Remote Sensing of Environment*, 113(6):1276–1292.

Pesaresi, M., and J.A. Benediktsson, 2001. A new approach for the morphological segmentation of high-resolution satellite imagery, *IEEE Transactions on Geoscience and Remote Sensing*, 39(2):309–320.

Prasad, A.M., L.R. Iverson, and A. Liaw, 2006. Newer classification and regression tree techniques: Bagging and random forests for ecological prediction, *Ecosystems*, 9(2):181–199.

Rosenfeld, A., and J.S. Weszka, 1976. *Picture Recognition*, Springer Berlin Heidelberg, pp. 135–166.

Schott, J.R., C. Salvaggio, and W.J. Volchok, 1988. Radiometric scene normalization using pseudoinvariant features, *Remote Sensing of Environment*, 26(1):1–16.

Sesnie, S.E., P.E. Gessler, B. Finegan, and S. Thessler, 2008. Integrating Landsat TM and SRTM-DEM derived variables with decision trees for habitat classification and change detection in complex neotropical environments, *Remote Sensing of Environment*, 112(5):2145–2159.

Serra, J., 1983. *Image Analysis and Mathematical Morphology*, Academic Press, Inc.

Sohl, T.L., 1999. Change detection in the United Arab Emirates: An investigation of techniques, *Photogrammetric Engineering & Remote Sensing*, 65(4):475–484.

Tobias, O.J., and S. Rui, 2002. Image segmentation by histogram thresholding using fuzzy sets, *IEEE Transactions on Image Processing*, 11(12):1457–1465.

Tuceryan, M., and A.K. Jain, 1998. Texture analysis, *Handbook of Pattern Recognition and Computer Vision* (C.H. Chen, L.F. Pau, and P.S.P. Wang, editors), World Scientific Publishing Co.

Tuia, D., F. Pacifici, M. Kanevski, and W.J. Emery, 2009. Classification of very high spatial resolution imagery using mathematical morphology and support vector machines, *IEEE Transactions on Geoscience and Remote Sensing*, 47(11):3866–3879.

Ye, S., and D. Chen, 2015. An unsupervised urban change detection procedure by using luminance and saturation for multispectral remotely sensed images, *Photogrammetric Engineering & Remote Sensing*, 81(8):637–645.

Youden, W.J., 1950. Index for rating diagnostic tests, *Cancer*, 3(1):32–35.

Zambon, M., R. Lawrence, A. Bunn, and S. Powell, 2006. Effect of alternative splitting rules on image processing using classification tree analysis, *Photogrammetric Engineering & Remote Sensing*, 72(1):25–30.

Zhang, L., X. Huang, B. Huang, and P. Li, 2006. A pixel shape index coupled with spectral information for classification of high spatial resolution remotely sensed imagery, *IEEE Transactions on Geoscience and Remote Sensing*, 44(10):2950–2961.

Zhang, R., D. Sun, Y. Yu, M.D. Goldberg, R. Zhang, and M.D. Goldberg, 2012. Mapping nighttime flood from MODIS observations using support vector machines, *Photogrammetric Engineering & Remote Sensing*, 78(11):1151–1161.

(Received 25 January 2016; accepted 18 April 2016; final version 18 November 2016)